

Violation of no-signaling on a public quantum computer

Tomasz Rybotycki^{1,2,3}, Tomasz Bialecki⁴, Josep Batle^{5,6,*} and Adam Bednorz^{4†}

¹*Systems Research Institute, Polish Academy of Sciences, 6 Newelska Street, PL01-447 Warsaw, Poland*

²*Nicolaus Copernicus Astronomical Center, Polish Academy of Sciences, 18 Bartycka Street, PL00-716 Warsaw, Poland*

³*Center of Excellence in Artificial Intelligence, AGH University,
30 Mickiewicza Lane, PL30-059 Cracow, Poland*

⁴*Faculty of Physics, University of Warsaw, ul. Pasteura 5, PL02-093 Warsaw, Poland*

⁵*Departament de Física and Institut d'Aplicacions Computacionals de Codi Comunitari (IAC3),
Campus UIB, E-07122 Palma de Mallorca, Balearic Islands, Spain and*

⁶*CRISP – Centre de Recerca Independent de sa Pobla, 07420 sa Pobla, Balearic Islands, Spain*

No-signaling is a consequence of the no-communication theorem that states that bipartite systems cannot transfer information unless a communication channel exists. It is also a by-product of the assumptions of Bell theorem about quantum nonlocality. We have tested no-signaling in bipartite systems of qubits from IBM Quantum devices in extremely large statistics, resulting in significant violations. Although the time and space scales of IBM Quantum cannot in principle rule out subluminal communications, there is no obvious physical mechanism leading to signaling. The violation is also at similar level as observed in Bell tests. It is therefore mandatory to check possible technical imperfections that may cause the violation and to repeat the loophole-free Bell test at much larger statistics, in order to be ruled out definitively at strict spacelike conditions.

I. INTRODUCTION

Quantum mechanics violates classical local realism, i.e. a counterfactual definite local hidden variable model generating measurement results [1]. It is shown by a Bell test [2], i.e. violation of a certain inequality, usually Clauser-Horne-Shimony-Holt (CHSH) [3] or Clauser-Horne [4], which requires at least two separated observers, each performing randomly chosen measurements. The important assumption of local realism is the lack of communication between them, i.e. one party does not know the choice of the other one before accomplishing its own measurement. This assumption cannot be verified *per se*, but its consequences can. The most prominent effect that can be tested is no-signaling, that is the result of the measurement of one party cannot depend on the choice of the other one. Note that it applies to single-party measurements, while two-party correlations can depend on both choices, which is the essence of the Bell test. The violation of Bell-type inequalities is a proof of entanglement only when the no-communication assumption is valid. The other way round, if no-signaling fails, so fails no-communication, and the Bell violation of local realism is meaningless. Since passing the Bell test is the ultimate proof of entanglement and rejection of local realism, it should be accompanied by a verified no-signaling test.

Experimental Bell tests have a long history of closing detection and communication loopholes [5–7]. Detection loophole means that the measurement is in fact trichotomic, not dichotomic, common in early optical experiments when the low efficiency of photodetectors lead to high percentage of lost photons, assigned to a third

outcome, and causing the whole event to be disregarded. To maintain the Bell conclusion fair sampling was assumed, i.e. the counted fraction is representative, not used to invent yet another local hidden variable model [8–11]. In other implementations, using superconductors, atoms and ions, it is never a problem as the outcome is always dichotomic [12–15], although auxiliary photons are sometimes preselected. In contrast to postselection, preselection is fully compatible with the Bell test, only lowering the overall statistics. Recent Bell experiments, even photonic, have the detection loophole closed [16, 17], but not all [18–20].

The lack of communication can be in principle ruled out by setting the observers, their choices and measurements, within a spatiotemporal framework. It is commonly assumed that the speed of light is the maximal speed of information transfer, but one has to remember that it does not simply follow from any, other than free, fundamental relativistic quantum field theory, because it is a nonperturbative claim [21]. It can be treated as an axiom, consistent with the general expectation of relativistic invariance of fundamental laws [22, 23].

To close the communication loophole, relying on the above axiom, the experimental setup requires sufficient spatial separation between observers so that the accomplished readout must lie outside of the forward causal lightcone created by the choice of the measurement of the other party, Fig. 1. Although it is compelling from the relativistic point of view, one can still check no-signaling. Certainly, if the axiom is valid, as commonly expected, the test should be passed. On the other hand, one can treat no-signaling as a confirmation, of rather lack of falsification, of relativity as regards communication limit. In the recent loophole-free experiments [24–28], no-signaling is routinely checked. Unfortunately, the present conclusion remains unclear [29]. A moderate violation of no-signaling occurs in the tests but has

* jbv276@uib.es, batlequantum@gmail.com

† Adam.Bednorz@fuw.edu.pl

never been checked more accurately [30, 31]. A collection of various Bell-type tests [32] revealed even more troubles [33]. In the first test on superconductors [15], no-signaling was violated by 70 standard deviations at extremely large number of trials, $\sim 34 \cdot 10^6$, attributed to measurement crosstalk at small distances. The recent loophole-free test [28] violates no-signaling at the p -value (probability that no-signaling hypothesis holds) of 2% [34] at ~ 250000 trials per a pair of choices. Both violations are of the same order so it is tempting to ask what if one reruns the latter test with a much larger number of trials.

Regarding relativity, it is treated as the ultimate bound on communication, although the physical description of the loophole-free setups is not directly relativistically covariant (light in the fibers/waveguide travels at about $2/3$ of the vacuum speed, due to collective interactions in the preferred reference frame) However, even at small distances and long times, any communication needs a reasonable physical origin, an appropriate propagating interaction. In this case violation of no-signaling is helpful in detection of unspecified communication channels and its analysis can reveal possible interaction mechanism.

Publicly available quantum computers, such as IBM Quantum, offer the real qubits (basic two-level systems, realized on transmons - superconducting Josephson junction shunted with capacitance) [35, 36] and gates (operation on a single qubit or a pair of them, realized by microwave pulses), [37–42]. Such a computer is expected to realize relatively faithfully the prepared sequences of operations, although they are often noisy, and cause some crosstalk. Nevertheless, the errors are quite well identified, by thermal noise, leakage to excited states or to the nearest neighbors. More complicated technical imperfections are expected to be so negligible that can be disregarded. The Bell-type tests can also be run on such computers [43–46], although the communication loophole in the relativistic sense remains open, due to small distances compared to the gate and measurement pulse times. Violation of no-signaling is a signature of either serious technical malfunction (e.g. short circuits in cables) or exotic physics behind the scenes.

In this work, we present the results of tests of no-signaling on IBM Quantum devices. They are composed of heavy hexagonal 127-qubit grids where each qubit is directly connected with one, two, or three other qubits. The connections allow to realize two-qubit gates to create entanglement and in principle to perform many-qubit operations transpiled into a sequence of native gates. We performed three types of experiments, testing signaling between next neighbors and fourth neighbors (parties separated by a chain of 3 other qubits). The nearest, direct, neighbors may affect each other by the connection. The experiments are:

- a) Bell test on next neighbors,
- b) idle test (i.e. local Bell measurements without any

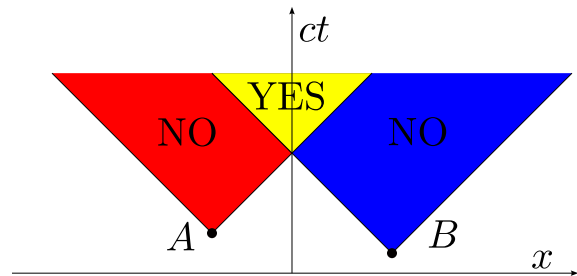


FIG. 1. Depiction of signaling (YES) and no-signaling regions (NO) in spacetime, here reduced to a single spatial dimension x , time t and speed of light c . The choices of A and B marked by black points are the apexes starting the forward causal lightcones (light triangles). Signaling only from A (B) is limited by relativistic causality axioms to the red (blue) region while the yellow part can receive signals from both parties. The remaining white region neither receives signals from A nor B . In the loophole-free Bell test, it is critical to accomplish the measurement within red and blue regions, for A and B observers, respectively.

entanglement) on next neighbors,

- c) idle test on fourth neighbors.

IBM Quantum allows to run tests simultaneously on several pairs of qubits, which is limited by possible path overlapping. We have found that: i) Bell inequality is violated in the majority of pairs in the test a), ii) no-signaling is violated in all a-b) tests but it is most prominent if qubit interlevel frequencies are similar, but still of lower order than Bell violation, iii) violation of no-signaling occurs also in c) but it is much smaller which sometimes requires larger statistics to increase confidence. In each test, we have found significant violations, at p -value below the threshold equivalent to 5 standard deviations, with additional borderline cases, that may become significant if continuing data collection.

Our paper is organized as follows. We start with the description of the circuits implemented on IBM Quantum for each test. Next, we present the results, both Bell and no-signaling tests. Then we explain the commonly suspected origins of signaling which fail to reproduce the observed violations. Finally some conclusions and discussion are drawn. Additional technical details are given in Appendix.

II. BELL AND NO-SIGNALING TESTS

Implementation of Bell and no-signaling tests on IBM Quantum relies on the grid of qubits, two-level systems with basis states $|0\rangle$ and $|1\rangle$, in energy eigenspace, differing by the energy $\hbar\omega$, where $f = \omega/2\pi$ is the drive frequency. They are manipulated by gates, operations on single or pairs of qubits. The states can be either pure $\rho = |\psi\rangle\langle\psi|$ or mixed, i.e. a convex normalized combination of pure states. Single qubit states are often rep-

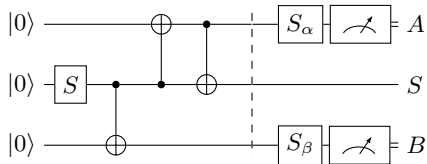


FIG. 2. Standard realization of the CHSH test on IBM Quantum for next neighbors in the test a). The gate S creates a superposition of $|0\rangle$ and $|1\rangle$ states on the source qubits S , entangled with the neighbor B by the $CNOT$ gate, and swapped by a pair of $CNOT$ s to the other neighbor A . The final measurements are the sequences of $Z_{\alpha/\beta}$ and S gates, $S_\alpha \equiv SZ_\alpha$. In the tests b-c), the entangling part left of the vertical dashed barrier are absent.

resented in the Bloch sphere $\rho = (1 + \boldsymbol{\sigma} \cdot \mathbf{v})/2$ for the set of Pauli matrices σ_k , $k = 1, 2, 3$ and vector $\mathbf{v} = (v_1, v_2, v_3)$ such that $|\mathbf{v}| \leq 1$.

A microwave pulse tuned to the interlevel drive frequency allows one to apply the parametrically controlled gates. The native single qubit gate we use is the $\pi/2$ rotation in Bloch sphere about the axis $(1, 0, 0)$

$$S = \sqrt{X} = (1 - i\sigma_1)/\sqrt{2} = \frac{1}{\sqrt{2}} \begin{pmatrix} 1 & -i \\ -i & 1 \end{pmatrix}, \quad (1)$$

in the $|0\rangle$, $|1\rangle$ basis. The auxiliary θ -rotation about $(0, 0, 1)$ axis, $Z(\theta)$, is a virtual operation, realized by a phase shift of the next gate, i.e.

$$S_\theta = Z_\theta^\dagger S Z_\theta, \quad Z_\theta = \begin{pmatrix} e^{-i\theta/2} & 0 \\ 0 & e^{i\theta/2} \end{pmatrix}. \quad (2)$$

In addition, there is a two-qubit $CNOT_\downarrow$ gate, operating as

$$|00\rangle\langle 00| + |01\rangle\langle 01| + |11\rangle\langle 10| + |10\rangle\langle 11|, \quad (3)$$

where for $|ab\rangle$ the control qubit states is a (depicted as \bullet) and target qubit state is b (depicted as \oplus in Fig. 2). The IBM Quantum devices use Echoed Crossed Resonance (ECR) gate, instead of $CNOT$ but one can transpile the latter by additional single-qubits gates, see Appendix A.

For the test a), we create an entangled state, applying S gate to the state $|0\rangle$ of the source qubit, to get $\sqrt{2}|\psi_0\rangle = |0\rangle - i|1\rangle$ and later $\sqrt{2}CNOT|\psi_0\rangle = |00\rangle - i|11\rangle$. We swap one of qubits to the neighbor by $CNOT_\downarrow CNOT_\uparrow|0\phi\rangle = |\phi 0\rangle$, which holds for an arbitrary $|\phi\rangle$.

The final Bell measurements A_a and B_b are performed by $SZ_\alpha \equiv S_\alpha$ on qubits A and S_β on qubit B , with the Bell angles $\alpha = 0, \pi/2$ for settings $a = 0, 1$ and $\beta = -\pi/4, \pi/4$ for settings $b = 0, 1$, respectively. The readout maps projectively the states for the values of observables A or B , $|0\rangle \rightarrow +1$ and $|1\rangle \rightarrow -1$ (we shall abbreviate $\pm 1 \rightarrow \pm$).

In the ideal case $\langle A \rangle = \langle B \rangle = 0$ while $\langle AB \rangle = -\sin(\alpha + \beta)$, for the average/correlation defined $\langle x \rangle_{ab} = \sum_x x P_{ab}(x)$ with the $P_{ab}(x)$ being the probability of the outcome x for settings ab .

	test entanglement	$A - B$ distance
a)	yes	2
b)	no	2
c)	no	4

TABLE I. Differences between of the tests a-c as regards the entanglement and distance.

The whole circuit is depicted in Fig. 2. We can construct CHSH inequality

$$CHSH = \sum_{ab} s_{ab} \langle AB \rangle_{ab} \leq 2, \quad (4)$$

$$s_{ab} = \begin{cases} +1 & \text{for } a = b = 0 \\ -1 & \text{otherwise} \end{cases}, \quad (5)$$

which is quantum violated at $2\sqrt{2} \simeq 2.818$.

The other tests do not contain the entangling part, just measurements, i.e. operations $S_{\alpha/\beta}$, with the same values $\alpha_{0,1} = 0, \pi/2$ and $\beta_{0,1} = -\pi/4, +\pi/4$ and the same or larger distance between A and B , as described in Table I.

The no-signaling test is performed as follows. In each of a-c) tests, we measure the probability $P_{ab}(AB)$, i.e. how often the pair of values AB are measured for a given pair of settings ab , and define single-party probability $P(A^*) = \sum_B P(AB)$, $P(*B) = \sum_A P(AB)$. No-signaling holds if

$$\begin{aligned} \delta P_{a*} &= P_{a0}(+) - P_{a1}(+), \\ \delta P_{*b} &= P_{0b}(+) - P_{1b}(+), \end{aligned} \quad (6)$$

are both equal to 0. For an ideal implementation $P(A^*) = P(*B) = 1/2$ regardless of AB and ab . Due to finite statistics, the probabilities are taken from the actual counts, i.e. $P(x) = N_x/N$, where N_x is the actual number for trials giving the outcome x out of N trials. It gives a possible error, which can be quantified, assuming independence of trials. For an equal number of trials N , we have

$$\begin{aligned} N\sigma^2 &= N\langle (\delta CHSH)^2 \rangle = \sum_{ab} (1 - \langle AB \rangle_{ab}^2), \\ N\sigma_{a*}^2 &= N\langle (\delta P_{a*})^2 \rangle = \sum_b P_{ab}(+)P_{ab}(-) \\ N\sigma_{*b}^2 &= N\langle (\delta P_{*b})^2 \rangle = \sum_a P_{ab}(+)P_{ab}(-) \end{aligned} \quad (7)$$

where $\delta CHSH = CHSH - CHSH$ for $CHSH$ equal the (5) from the actual statistics. The error is crucial to identify significance of the potential violation of Bell inequality or no-signaling. In addition, one can express the significance in terms of p -value, i.e. the probability that the local realism or no-signaling hypothesis holds. For a single test it is calculated as the double tail of the Gaussian probability distribution with the above standard deviations, i.e events below $-|z|$ and above $+|z|$ for

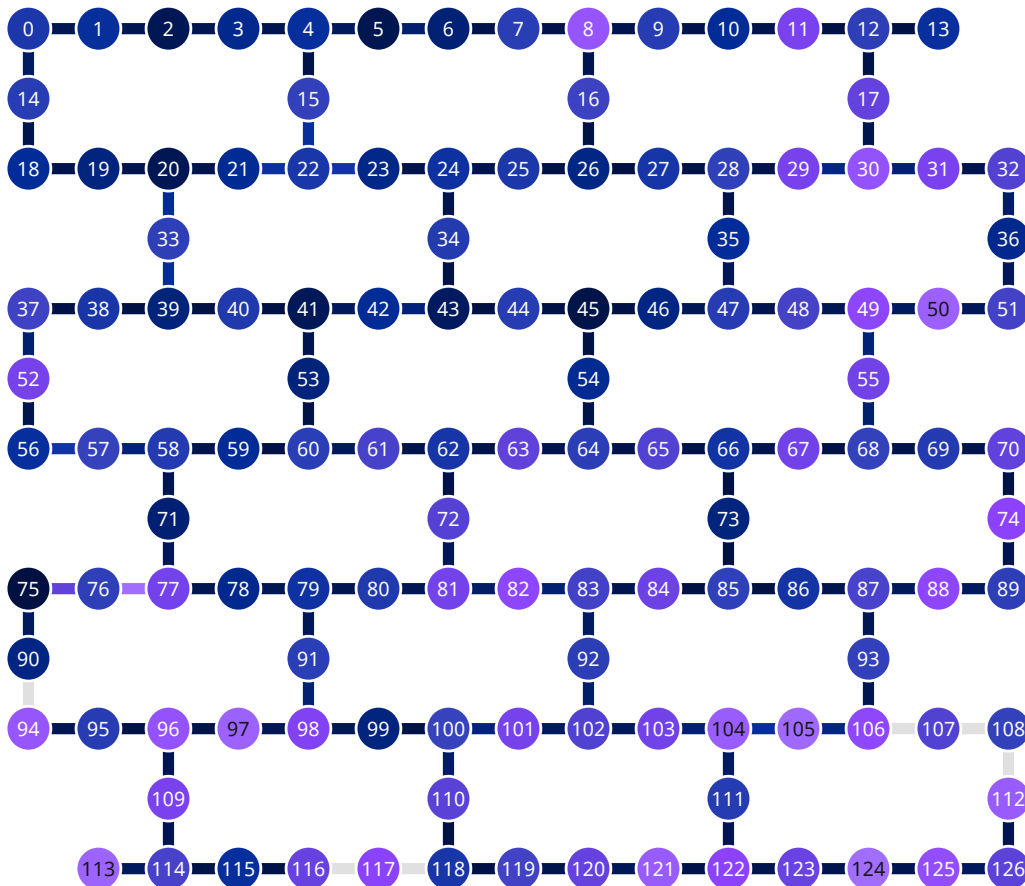


FIG. 3. Topology of the qubit grid of IBM Quantum devices in Eagle generation, *ibm_sherbrooke*, *ibm_brisbane*, *ibm_kyoto*, *ibm_kyiv*. Here the circles represent qubits, bars connections for two-qubit gates. The grid is actually hexagonal.

the z score, corresponding to the actually observed value of $CHSH - 2$ or δP , i.e.

$$p(z) = 2 \int_z^\infty e^{-z^2/2\sigma^2} / \sqrt{2\pi\sigma^2} = \text{erfc}(z/\sqrt{2}\sigma). \quad (8)$$

The actual p -value is taken from the above formula, but multiplied by the number of possible tests, also known as Bonferroni corrections of look-elsewhere effect [47, 48].

III. RESULTS

IBM Quantum allows to run experiments in single units, jobs. Each job consists of a sequence of circuits, which can be different. Each circuit corresponds to an individual experiment run, as specified in the previous section, i.e. a sequence of gates ending with measurements. The standard time for a single run is 250 microseconds. Each sequence of circuits is repeated by the number of shots.

We have run tests a-b) on the same sets of qubits, on Eagle generation *ibm_sherbrooke*, *ibm_brisbane*, *ibm_kyoto*, with 20000 shots, 60 jobs, *ibm_kyiv* with 7500 shots (due to slower operation), 58 and 60 jobs

for test a) and b) respectively, and 25 repetitions for each choice configuration ab , randomly shuffled, giving the total number of circuits 100. We tested simultaneously several non-overlapping pairs of next-neighbor qubits. We have depicted the topology of IBM Quantum devices in Fig. 3. It gives the total number of trials $3 \cdot 10^7$ (except $\sim 10^7$ for *ibm_kyiv*). The tests c) on the same devices, have been run with the same number of jobs (60 for *emph_kyiv*), shots and repetitions, except *ibm_sherbrooke*, where the number of jobs was 240. The results of Bell and no-signaling tests are given in Tables II,III,IV,V,VI,VII,VIII,IX. The standard deviation in almost all tests is roughly the same, $1.3 \cdot 10^{-4}$, except c) on *ibm_sherbrooke*, $6.4 \cdot 10^{-5}$. The jobs were run in August 2024, except b) and c) for *ibm_kyiv* in September 2024, each job takes about 530 seconds. The total run time was several hours, except c) on *ibm_sherbrooke*, which was about 3 days. During the test, the devices underwent routine calibrations, which do not affect the experiment, as the test is linear. In particular, the qubit drive frequencies may vary at the relative level $\sim 10^{-6}$.

It turns out that the majority of tests a) confirm violation of Bell-CHSH inequality, but a-b) also often violate no-signaling. The violation of no-signaling is the

$A - S - B$	a) CHSH	σ	δP_{0*}	δP_{1*}	δP_{*0}	δP_{*1}	b) δP_{0*}	δP_{1*}	δP_{*0}	δP_{*1}	f_{A-B}
55-68-67	2.25	3.0	103	281	104	-64.2	-93.9	-227	-185	-87.6	0.77
34-43-44	2.4	3.0	70.8	63.3	85	84.3	26.4	-112	-59	19.1	-4.2
29-30-31	1.84	3.2	-12.6	6.32	-0.617	-20.3	-25	88.2	89	-23.1	-5.5
101-102-103	2.15	3.0	-50.1	-76	-63.7	-28.3	-73.2	10.2	62.7	-71.9	6.8
7-8-9	1.6	3.0	-40.9	-12.7	-13.9	-47.1	4.55	-3.02	-2.75	3.75	8.2
74-89-88	2.26	2.8	2	-2.78	-0.305	3.11	-1.87	-14.2	7.85	34.4	-9.3
94-95-96	2.14	3.0	8.74	6.7	3.98	3.28	-7.87	-5.25	-4.35	-17.6	15
25-26-27	2.37	3.0	2.37	-6.63	-1.91	8.89	7.83	10.5	1.53	16.3	15
63-62-72	2.45	2.8	0.569	-0.013	-1.11	0.904	-3.24	2.93	4.9	-4.48	17
38-39-40	2.34	2.8	0.0717	-7.03	-8.67	-9.78	-0.827	1.72	0.814	4.08	-17
58-59-60	2.28	3.0	1.8	-1.53	-1.67	5.53	14	2.87	5.38	18.6	-20
21-22-23	1.59	3.4	2.92	-1.69	-0.678	3.76	-0.112	5.26	7.78	-0.222	21
80-79-91	2.19	3.0	0.352	1.55	4.17	2.34	1.94	-0.324	0.962	-0.988	-26

TABLE II. Results of the test a) and b) for *ibm_kyoto*, qubits A and B as specified, with the source qubits S (middle). Here, all σ and δP are in units 10^{-4} while $f_{A-B} = f_A - f_B$ is the frequency difference between qubit A and B in MHz. The error $\sigma_{a*}, \sigma_{*b} \simeq 1.3 \cdot 10^{-4}$. We have highlighted in bold the strongest violations of no-signaling.

$A - S - B$	a) CHSH	σ	δP_{0*}	δP_{1*}	δP_{*0}	δP_{*1}	b) δP_{0*}	δP_{1*}	δP_{*0}	δP_{*1}	f_{A-B}
1-2-3	1.68	3.2	-4.21	0.275	-10.6	2.34	-1.09	-0.531	-0.24	-0.709	-60
7-8-9	2.15	2.8	0.072	21.6	19.8	4.54	-1.32	17.4	9.61	6.68	-20
11-12-13	2.06	3.2	10.4	-2.88	-3.08	0.688	-0.663	-2.76	-0.184	0.108	-34
39-40-41	2.38	2.8	-2.44	-1.87	-3.14	-3.63	9.75	9.53	7.08	5.34	-18
44-45-46	2.31	3.0	-7.11	0.813	8.66	0.149	-3.55	0.577	0.951	0.882	96
67-68-69	1.68	3.2	-55.7	38.5	17	-75.9	-37.6	-14.6	-46	-47.5	-3.7
79-80-81	1.61	3.2	4.46	-2.55	7.57	-3.06	-1.62	-0.248	1.64	-2.14	-67
83-84-85	2.39	3.0	-8.1	-0.238	0.447	-1	-2.17	1.65	-1.53	1.08	-310
95-96-97	2.18	3.0	-6.06	-1.76	1.54	-6.21	-2.48	3.84	6.44	-1.96	23
106-107-108	2.01	3.3	-0.104	-0.445	-6.61	1.63	-0.55	2.37	-1.05	-3.26	-180
113-114-115	1.94	3.3	78.8	114	94	56.6	32.5	71.4	58.9	28	4
122-123-124	2.44	2.8	-10.6	-31.8	-25.2	-2.62	-6.79	54	24.8	-14.6	-12

TABLE III. Results of the test a) and b) for *ibm_brisbane*, notation as in Table II

strongest when the frequencies of A and B are similar, but it still happens in some cases with large frequency difference, e.g. 80-82 on *ibm_sherbrooke* and 44-46 on *ibm_brisbane* with differences 230 and 96 MHz, respectively. In all tests c) there are also pairs violating no-signaling, but the violation is smaller, although it seems that still larger at small frequency difference.

We have additionally analyzed the extreme case of test c), *ibm_sherbrooke* pair 49-66, checking the probability, Table X, and results of δP for individual jobs, Fig. 4. No accidental violation has been found, although the violation may get some drift over time. The p -value is $5.3 \cdot 10^{-17}$, taking into account estimating $127 \cdot 8$ possible pairs by the look elsewhere effect, compared to the agreed border at 5 standard deviations, $5.7 \cdot 10^{-7}$. The data and scripts are available publicly [51].

IV. ANALYSIS OF TECHNICAL IMPERFECTIONS

The observed violations of no-signaling are significant, but vary between different qubits pairs. It is tempting

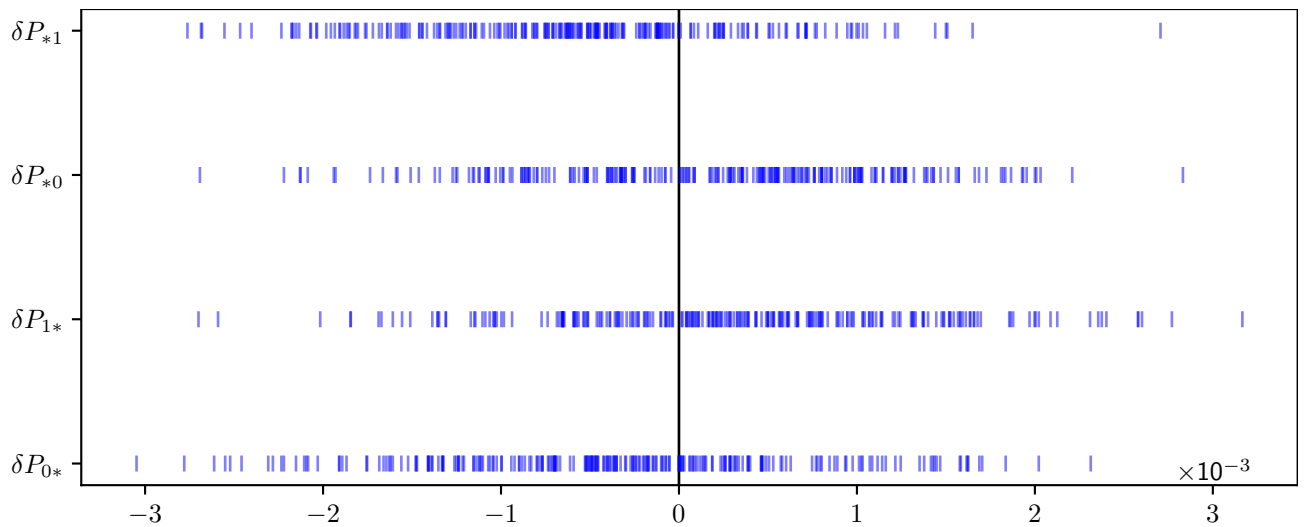
to seek for the origin in technical imperfections of IBM Quantum devices. It is known that frequency collisions lead to serious crosstalk, but usually due to two-qubit gates driven by the neighbor's frequency, or heating disturbance [52, 53]. Certainly the measurement times of > 1 microsecond compared to the distances of several cm allows communication in the relativistic sense. However, there are no obvious interactions responsible for it. The most natural ZZ crosstalk, i.e. the interaction diagonal in the energy basis of the set of qubits, does not help, as $S_{\alpha/\beta}$ differ only by the phase. Even if the qubits have similar frequencies, they are not exactly equal and the phases are not synchronized.

If one insists on technical explanations, they must be much more tricky. An error of S gate is insufficient if the Z gate (phase shift) works correctly. It is the Z gate that must be erroneous, which means an error at the time of pulse preparation. The microwave pulse is formed by combining Arbitrary Waveform Generator (AWG), Local Oscillator (LO) generating continuous wave of the qubit drive frequency and in-phase/quadrature mixer (IQM), i.e. the device that combines signals of phase shifted by $\pi/2$ [49], see Fig. 5. If the effect is correlation of

$A - S - B$	a) CHSH	σ	δP_{0*}	δP_{1*}	δP_{*0}	δP_{*1}	b) δP_{0*}	δP_{1*}	δP_{*0}	δP_{*1}	f_{A-B}
4-5-6	2.06	3.2	2.66	-0.795	-6.22	2.16	2.38	1.02	0.362	-2.15	-110
11-12-13	2.25	3.0	1.6	0.38	1.35	0.881	-2.08	3.33	-1.39	-1.66	190
21-22-23	1.57	3.4	13.9	14.4	9.63	13	-6.15	4.48	8.44	-6.7	16
28-29-30	2.23	3.0	-22.5	6.73	2.41	0.217	0.156	-0.5	0.324	0.338	51
37-38-39	2.41	2.8	8.58	8.94	3.52	-0.321	-1.71	-11.1	-10.1	0.926	20
43-44-45	2.54	2.8	4.65	-82.3	-4.03	87.2	48.1	56	59.2	52.7	-7.7
47-48-49	2.6	2.8	-4.1	-12.7	-18.5	-14.5	-5.13	-11.6	-7.11	-7.94	-16
60-61-62	2.31	3.0	0.306	-1.53	-1.2	-0.15	0.958	-0.0307	-1.05	-1.51	-99
80-81-82	1.24	3.4	21	-8.86	0.435	-0.775	-0.627	-0.605	-2.56	1.93	230
94-95-96	2.06	3.0	1.34	-1.12	1.43	-0.204	0.021	1.79	1.52	2.29	-130
102-103-104	2.55	2.8	133	198	101	29.9	-12.7	152	159	-12.3	2.8
117-118-119	2.53	2.8	313	510	306	103	-295	249	242	-308	0.43
123-124-125	2.49	2.8	-2.02	0.874	-1.38	-1.02	1.46	2.27	-1.22	0.827	-160

TABLE IV. Results of the test a) and b) for $ibm_sherbrooke$, notation as in Table II

$A - S - B$	a) CHSH	σ	δP_{0*}	δP_{1*}	δP_{*0}	δP_{*1}	b) δP_{0*}	δP_{1*}	δP_{*0}	δP_{*1}	f_{A-B}
11-12-13	2.36	4.8	-40.7	109	0.0432	-145	-115	-61.9	-70	-109	-1.8
80-81-82	1.82	5.4	123	184	184	106	-17.2	140	167	-32.2	-1.8
24-25-26	2.39	4.8	-166	-85.2	-191	-272	-91.4	186	197	-82.4	-2.6
31-32-36	2.33	5.0	22.5	-23.2	17.1	65.5	14.3	-51.5	-42.8	12.9	5
92-102-101	2.6	4.6	-12.7	-66.6	-7.44	53.3	3.34	61.3	60.6	-0.008	5.2
9-8-16	2.16	5.0	-4.21	-12.2	-8.86	2.11	-21.3	22.6	28.2	-20.6	5.8
38-39-40	2.21	5.0	-5.75	-34.9	-1.25	24.6	-69.2	21.8	19.2	-81.1	-5.8
77-78-79	2.17	5.0	-30.6	-12.5	-49.3	-71.6	-42.7	25.2	26	-49.7	5.9
54-64-63	2.5	4.8	-63.1	-17.4	-78	-111	-58.3	-70.6	-63.8	-49.6	-6.1
123-124-125	2.13	5.0	58.7	64.7	67	64.9	37.7	2.48	5.58	43.9	-6.5
84-85-86	1.61	5.0	6.63	8.89	9.27	4.54	-10.5	20.3	13.5	-6.92	-6.8
119-120-121	2.07	5.2	46.9	36.6	45.7	57.2	-26.3	31.3	31.4	-19.1	-9.6
15-22-21	2.41	4.8	-1.11	2.02	-2.56	-3.84	-8.84	-3.21	-6.3	-20.5	11

TABLE V. Results of the test a) and b) for ibm_kyiv , notation as in Table II, except error. The error $\sigma_{a*}, \sigma_{*b} \simeq 2.14 \cdot 10^{-4}$, and $2.1 \cdot 10^{-4}$, in test a) and b) respectively.FIG. 4. Signaling defined by Eq. (6) calculated in the test c) on $ibm_sherbrooke$ pair $A - B : 49 - 66$ for each individual job, i.e. each bar corresponds to the value calculated for a single job, out of 240.

$A - B$	δP_{0*}	δP_{1*}	δP_{*0}	δP_{*1}	f_{A-B}
11-31	2.73	0.531	1.03	-1.08	-0.06
77-81	-3.43	1.46	-0.557	-1.12	0.073
42-59	1.35	-0.644	0.909	-1.69	-1.6
116-120	22.3	23.3	-22.8	24.4	3.7
68-85	-36.8	-0.803	19.6	-3.17	8.8
15-33	-16.7	-9.9	5.57	-0.193	5.7
84-103	-3.09	9.67	-1.39	17.6	-6.3
97-113	10	14.4	35.7	-5.35	-7.1

TABLE VI. Results of the test c) for *ibm_kyoto*, notation as in Table II

$A - B$	δP_{0*}	δP_{1*}	δP_{*0}	δP_{*1}	f_{A-B}
41-62	-0.425	-0.0373	-0.935	0.216	0.32
76-95	2.2	0.705	1.12	1.81	-1.5
15-25	-2.18	-0.307	0.982	1.38	2.8
7-11	3.52	-2.21	-1.65	-0.457	-4.8
28-45	-11.4	-25.5	20.3	-2.42	-5
82-86	-0.231	-0.626	0.86	0.168	-5.2
111-125	-0.417	1.7	-4.02	-0.802	-6
100-116	-10.6	-1.02	9.64	-10.9	-7.4

TABLE VII. Results of the test c) for *ibm_brisbane*, notation as in Table II

phase with the pulse amplitude error, the subsequent ZZ crosstalk may cause signaling. On the other hand, amplitude error would lead to significant local error, i.e. much more significant change of the qubit directly controlled, not the other party, which we do not observe.

Another brute explanation is a short circuit between cables already before reaching AWG. We refrain from such drastic claims, as most experiments, even loophole-free Bell tests, rely on the trust in experimental setup. If one cannot take for granted the reliable process of the local choice and the time of measurement accomplishments, no conclusions can be drawn from any experiments. On the other hand, problems with cables and timings sometimes do become an issue [50].

$A - B$	δP_{0*}	δP_{1*}	δP_{*0}	δP_{*1}	f_{A-B}
109-117	-0.284	0.59	-0.0604	-0.775	0.99
49-66	-3.36	3.29	1.86	-5.89	1.2
68-85	0.102	-0.244	-1.39	0.109	-4
92-99	-0.456	0.542	-0.705	-1.7	-4.7
34-40	0.293	0.81	0.421	-0.00325	5.2
27-46	2.22	-0.283	-0.376	-1.04	6.3
120-124	1.53	-1.51	-3.8	1.33	6.5
52-71	0.877	-0.484	0.247	0.665	8.6

TABLE VIII. Results of the test c) for *ibm_sherbrooke*, notation as in Table II, except that here $\sigma_{a*}, \sigma_{*b} \simeq 6.4 \cdot 10^{-5}$

$A - B$	δP_{0*}	δP_{1*}	δP_{*0}	δP_{*1}	f_{A-B}
97-110	-3.38	-1.41	-0.692	-2.15	0.87
26-30	3.42	1.92	-0.00711	0.307	2.2
3-14	-0.0507	5.28	-3.34	-1.58	2.6
62-66	2.1	-3.9	-3.46	-2.37	-3.6
43-60	1.06	-0.298	1.51	-0.499	5.5
105-123	0.185	2.29	-3.87	3.44	9.3
18-39	-32.3	26.1	-8.65	1.48	10
6-10	2.88	-0.268	-1.15	-0.723	12

TABLE IX. Results of the test c) for *ibm_kyiv*, notation as in Table II, except that here $\sigma_{a*}, \sigma_{*b} \simeq 2.1 \cdot 10^{-4}$.

ab	$P(++)$	$P(+-)$	$P(-+)$	$P(--)$	$P(+*)$	$P(*+)$
00	0.27779	0.22945	0.26979	0.22297	0.50724	0.54758
10	0.28060	0.23202	0.26679	0.22059	0.51262	0.54740
01	0.27800	0.22958	0.26975	0.22267	0.50758	0.54775
11	0.28092	0.23137	0.26742	0.22029	0.51229	0.54834

TABLE X. Probabilities for $P_{ab}(AB)$ for the test c) on *ibm_sherbrooke* pair $A - B : 49 - 66$

V. DISCUSSION

We have checked Bell inequality and no-signaling on IBM Quantum devices. It turns out that although Bell violation is observed, there is also violation of no-signaling. The violation of no-signaling is large and cannot be explained by a simple crosstalk. The level of the violation is similar to other superconducting experiments [15, 28], at very high statistics. It is urgent to resolve the origin of the violation. Other tests, possibly in different configuration or implementation, should be run. Also, the loophole-free Bell experiment [28] should be also re-run at larger number of trials and various configurations (also idle, and various sets of angles). It is certainly difficult to quantify the consequences that these errors may entail in more involved experiments, or how they propagate when global multiqubit tasks are involved. Thus, a thorough further technical analysis to ascertain the ex-

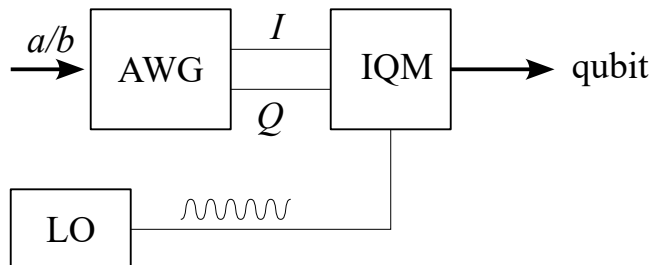


FIG. 5. The signal flow from the choice a/b to the actual qubits drive pulse. The AWG creates a pulse amplitude with its in-phase I and quadrature Q component. The LO creates the continuous wave of the qubit drive frequency. The IQM combines the two waves into a single microwave pulse fed to the qubit.

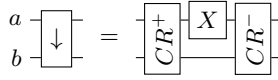


FIG. 6. The notation of the ECR gate in the convention $ECR_{\downarrow}|ab\rangle$

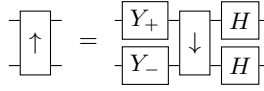


FIG. 7. The ECR_{\uparrow} gate expressed by ECR_{\downarrow}

act source of errors is absolutely imperative for future endeavors. Unless one resolves these issues, more exotic, fundamental explanations involving extra states beyond simple models predicting extra dimensions, as many worlds/copies [54, 55], must be considered.

ACKNOWLEDGMENTS

The results have been created using IBM Quantum. The views expressed are those of the authors and do not reflect the official policy or position of the IBM Quantum team. We thank Jakub Tworzydło for advice, technical support, and discussions, Stanisław Sołtan for the discussion about frequency collisions, and Witold Bednorz for consultations on error analysis. TR gratefully acknowledges the funding support by the program „Excellence initiative research university” for the AGH University in Krakow as well as the ARTIQ project: UMO-2021/01/2/ST6/00004 and ARTIQ/0004/2021. We also thank Bartłomiej Zglinicki and Bednorz family for the support.

Appendix A: Relation between $CNOT$ and ECR gates

The IBM Quantum devices use a native two-qubit ECR instead of $CNOT$ [39, 40] but one can transpile the latter by the former, adding single qubits gates. We shall use Pauli matrices in the basis $|0\rangle, |1\rangle$,

$$X = \begin{pmatrix} 0 & 1 \\ 1 & 0 \end{pmatrix}, Y = \begin{pmatrix} 0 & -i \\ i & 0 \end{pmatrix}, Z = \begin{pmatrix} 1 & 0 \\ 0 & -1 \end{pmatrix}, I = \begin{pmatrix} 1 & 0 \\ 0 & 1 \end{pmatrix}. \quad (\text{A1})$$

We also denote two-qubits gates by \downarrow and \uparrow , which mean the direction of the gate (it is not symmetric), i.e. $\langle a'b'|G_{\uparrow}|ab\rangle = \langle b'a'|G_{\downarrow}|ba\rangle$.

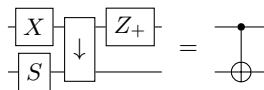


FIG. 8. The $CNOT_{\downarrow}$ gate expressed by ECR_{\downarrow}

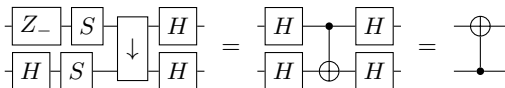


FIG. 9. The $CNOT_{\uparrow}$ gate expressed by ECR_{\downarrow}

The ECR gate acts on the states $|ab\rangle$ as (Fig. 6)

$$ECR_{\downarrow} = (XI - YX)/\sqrt{2} = CR^{-}(XI)CR^{+} = \begin{pmatrix} 0 & X_{-} \\ X_{+} & 0 \end{pmatrix} = \begin{pmatrix} 0 & 0 & 1 & i \\ 0 & 0 & i & 1 \\ 1 & -i & 0 & 0 \\ -i & 1 & 0 & 0 \end{pmatrix} / \sqrt{2}, \quad (\text{A2})$$

in the basis $|00\rangle, |01\rangle, |10\rangle, |11\rangle$ where the native gate is

$$S = X_{+} = X_{\pi/2} = (I - iX)/\sqrt{2} = \begin{pmatrix} 1 & -i \\ -i & 1 \end{pmatrix} / \sqrt{2}, \quad (\text{A3})$$

and $X_{-} = X_{-\pi/2} = ZX_{+}Z$, with

$$CR^{\pm} = (ZX)_{\pm\pi/4}, \quad (\text{A4})$$

using the convention $V_{\theta} = \exp(-i\theta V/2) = \cos(\theta/2) - iV \sin(\theta/2)$ if $V^2 = I$ or II . The gate is its inverse, i.e. $ECR_{\downarrow}ECR_{\downarrow} = II$.

Note that $Z_{\theta} = \exp(-i\theta Z/2) = \text{diag}(e^{-i\theta/2}, e^{i\theta/2})$ is a virtual gate adding essentially the phase shift to next gates. ECR gates can be reversed, i.e., for $a \leftrightarrow b$, (Fig. 7)

$$ECR_{\uparrow} = (IX - XY)/\sqrt{2} = (HH)ECR_{\downarrow}(Y_{+}Y_{-}), \quad (\text{A5})$$

denoting $V_{\pm} = V_{\pm\pi/2}$, and Hadamard gate,

$$H = (Z + X)/\sqrt{2} = Z_{+}SZ_{+} = \begin{pmatrix} 1 & 1 \\ 1 & -1 \end{pmatrix} / \sqrt{2}, \quad (\text{A6})$$

and $Z_{\pm}SZ_{\mp} = Y_{\pm}$, with $Y_{+} = HZ$ and $Y_{-} = ZH$.

The $CNOT$ gate can be expressed by ECR (Fig. 8)

$$CNOT_{\downarrow} = (II + ZI + IX - ZX)/2 = \begin{pmatrix} I & 0 \\ 0 & X \end{pmatrix} = \begin{pmatrix} 1 & 0 & 0 & 0 \\ 0 & 1 & 0 & 0 \\ 0 & 0 & 0 & 1 \\ 0 & 0 & 1 & 0 \end{pmatrix} = (Z_{+}I)ECR_{\downarrow}(XS), \quad (\text{A7})$$

while its reverse reads (Fig. 9)

$$CNOT_{\uparrow} = (II + IZ + XI - XZ)/2 = \begin{pmatrix} 1 & 0 & 0 & 0 \\ 0 & 0 & 0 & 1 \\ 0 & 0 & 1 & 0 \\ 0 & 1 & 0 & 0 \end{pmatrix} = (HH)CNOT_{\downarrow}(HH) = (HH)ECR_{\downarrow}(SS)(Z_{-}H). \quad (\text{A8})$$

- [1] A. Einstein, B. Podolsky, N. Rosen, Can Quantum-Mechanical Description of Physical Reality Be Considered Complete?, *Phys. Rev.* **47**, 777 (1935).
- [2] J.S. Bell, On the Einstein Podolsky Rosen paradox, *Physics* (Long Island City, N.Y.) **1**, 195 (1964); A. Shimony, Bell's Theorem, plato.stanford.edu/entries/bell-theorem/.
- [3] J.F. Clauser, M.A. Horne, A. Shimony and R.A. Holt, Proposed Experiment to Test Local Hidden-Variable Theories *Phys. Rev. Lett.* **23**, 880(1969).
- [4] John F. Clauser and Michael A. Horne, Experimental consequences of objective local theories *Phys. Rev. D* **10**, 526 (1974). P.H. Eberhard, Background level and counter efficiencies required for a loophole-free Einstein-Podolsky-Rosen experiment, *Phys. Rev. A* **47**, R747 (1993).
- [5] P.M. Pearle, Hidden-Variable Example Based upon Data Rejection, *Phys. Rev. D* **2**, 1418 (1970).
- [6] E. Santos, Critical analysis of the empirical tests of local hidden-variable theories, *Phys. Rev. A* **46**, 3646 (1992).
- [7] J.-A. Larsson, Loopholes in Bell inequality tests of local realism, *J Phys. A* **47**, 424003 (2014).
- [8] A. Aspect, J. Dalibard, G. Roger, Experimental Test of Bell's Inequalities Using Time-Varying Analyzers, *Phys. Rev. Lett.* **49**, 1804 (1982).
- [9] G. Weihs, T. Jennewein, C. Simon, H. Weinfurter, A. Zeilinger, Violation of Bell's Inequality under Strict Einstein Locality Conditions *Phys. Rev. Lett.* **81**, 5039 (1998).
- [10] W. Tittel, J. Brendel, H. Zbinden, N. Gisin, Violation of Bell Inequalities by Photons More Than 10 km Apart, *Phys. Rev. Lett.* **81**, 3563 (1998).
- [11] T. Scheidl *et al.*, Violation of local realism with freedom of choice, *Proc. Natl. Acad. Sci. U.S.A.* **107**, 19708 (2010).
- [12] J. Hofmann *et al.*, Heralded entanglement between widely separated atoms, *Science* **337**, 72 (2012).
- [13] M.A. Rowe *et al.*, Experimental violation of a Bell's inequality with efficient detection, *Nature* **409**, 791 (2001).
- [14] D.N. Matsukevich, P. Maunz, D.L. Moehring, S. Olmschenk, C. Monroe, Bell Inequality Violation with Two Remote Atomic Qubits, *Phys. Rev. Lett.* **100**, 150404 (2008).
- [15] A. Ansmann *et al.*, Violation of Bell's inequality in Josephson phase qubits, *Nature* **461**, 504 (2009).
- [16] M. Giustina *et al.*, Bell violation using entangled photons without the fair-sampling assumption, *Nature* **497**, 227-230 (2013).
- [17] B.G. Christensen *et al.*, Detection-Loophole-Free Test of Quantum Nonlocality, and Applications, *Phys. Rev. Lett.* **111**, 130406 (2013).
- [18] J. Handsteiner *et al.*, Cosmic Bell Test: Measurement Settings from Milky Way Stars, *Phys. Rev. Lett.* **118**, 060401 (2017).
- [19] D. Rauch *et al.*, Cosmic Bell Test using Random Measurement Settings from High-Redshift Quasars, *Phys. Rev. Lett.* **121**, 080403 (2018).
- [20] Y. Liu *et al.*, Experimental measurement-dependent local Bell test with human free will, *Phys. Rev. A* **99**, 022115 (2019)
- [21] A. Bednorz, Objective realism and freedom of choice in relativistic quantum field theory, *Phys. Rev. D* **94**, 085032 (2016).
- [22] R. F. Streater and A. S. Wightman, PCT, spin and statistics, and all that (Benjamin, New York, 1964).
- [23] A. Bednorz, Relativistic invariance of the vacuum, *Eur. Phys. J. C* **73**, 2654 (2013).
- [24] B. Hensen, *et al.*, Loophole-free Bell inequality violation using electron spins separated by 1.3 kilometres, *Nature* **526**, 682 (2015).
- [25] L.K. Shalm *et al.*, Strong Loophole-Free Test of Local Realism, *Phys. Rev. Lett.* **115**, 250402 (2015).
- [26] M. Giustina *et al.*, Significant-Loophole-Free Test of Bell's Theorem with Entangled Photons, *Phys. Rev. Lett.* **115**, 250401 (2015).
- [27] W. Rosenfeld *et al.*, Event-Ready Bell Test Using Entangled Atoms Simultaneously Closing Detection and Locality Loopholes, *Phys. Rev. Lett.* **119**, 010402 (2017).
- [28] S. Storz *et al.*, Loophole-free Bell inequality violation with superconducting circuits, *Nature* **617**, 265 (2023).
- [29] M. Smania, M. Kleinmann, A. Cabello, M. Bourennane, Avoiding apparent signaling in Bell tests for quantitative applications, arXiv:1801.05739
- [30] A. Bednorz, Analysis of assumptions of recent tests of local realism, *Phys. Rev. A* **95**, 042118(2017)
- [31] G. Adenier, A. Yu. Khrennikov, Test of the no-signaling principle in the Hensen loophole-free CHSH experiment, *Fortschr. der Physik* **65**, 1600096 (2017); D.A. Graft, Rhetoric, logic, and experiment in the quantum nonlocality debate, *Open Physics* **15**, 586 (2017)
- [32] The Big Bell Test Collaboration, Challenging local realism with human choices, *Nature* **557**, 212(2018)
- [33] S. Sołtan, D. Dopierała, A. Bednorz, Analysis of Assumptions in BIG Bell Test Experiments. *Annalen der Physik* **532**, 2000333 (2020).
- [34] There is a typo in [28] in Table SVI, missing 0 after period in rows 2 and 4.
- [35] J. Koch, Terri M. Yu, J. Gambetta, A. A. Houck, D. I. Schuster, J. Majer, Alexandre Blais, M. H. Devoret, S. M. Girvin, R. J. Schoelkopf, Charge-insensitive qubit design derived from the Cooper pair box, *Phys. Rev. A* **76**, 042319 (2007).
- [36] J. M. Gambetta, J. M. Chow, and M. Steffen, *Building logical qubits in a superconducting quantum computing system* npj Quantum Inf. **3**, 2 (2017).
- [37] F. Motzoi, J. M. Gambetta, P. Rebentrost, and F. K. Wilhelm, Simple Pulses for Elimination of Leakage in Weakly Nonlinear Qubits *Phys. Rev. Lett.* **103**, 110501 (2009).
- [38] J. M. Gambetta, F. Motzoi, S. T. Merkel, and F. K. Wilhelm, Analytic control methods for high-fidelity unitary operations in a weakly nonlinear oscillator, *Phys. Rev. A* **83**, 012308 (2011).
- [39] M. Malekakhlagh, E. Magesan, and D. C. McKay. First-principles analysis of cross-resonance gate operation, *Phys. Rev. A* **102**, 042605 (2020).
- [40] E. Magesan and J. M. Gambetta, Effective Hamiltonian models of the cross-resonance gate, *Phys. Rev. A* **101**, 052308 (2020).
- [41] IBM Quantum Platform, quantum.ibm.com
- [42] <https://qiskit.org/textbook>
- [43] D. Alsinga, I. Latorre, Experimental test of Mermin in-

- equalities on a five-qubit quantum computer, Phys. Rev. A **94**, 012314 (2016).
- [44] D. Garcia-Martin and G. Sierra, Five Experimental Tests on the 5-Qubit IBM Quantum Computer, J. Appl. Math. and Phys. **6**, 1460 (2018).
- [45] IBM Quantum Learning, Tutorial: CHSH Inequality, learning.quantum.ibm.com/tutorial/chsh-inequality
- [46] J. Brody, R. Avram, Testing a Bell Inequality with a Remote Quantum Processor, Phys. Teach. **61**, 218 (2023).
- [47] C. E. Bonferroni, Teoria statistica delle classi e calcolo delle probabilita, Pubblicazioni del R Istituto Superiore di Scienze Economiche e Commerciali di Firenze 1936; O.J. Dunn, Estimation of the Medians for Dependent Variables, Ann. of Math. Statistics. **30**, 192 (1959); Multiple Comparisons among Means, J. of the Am. Stat. Association. **56**, 52 (1961)
- [48] L. Lyons, Open statistical issues in Particle Physics, Ann. Appl. Stat. **2**, 887 (2008); S. Chatrchyan *et al.* (CMS Collaboration), Search for Three-Jet Resonances in $p p$ Collisions at $\sqrt{s} = 7$ TeV Phys. Rev. Lett. **107**, 101801 (2011), Synopsis, Controlling for the "look-elsewhere effect", E. Gross, O. Vitells, Trial factors for the look elsewhere effect in high energy physics, Eur. Phys. J. C **70**, 525 (2010).
- [49] D. C. McKay, C. J. Wood, S. Sheldon, J. M. Chow, J. M. Gambetta, Efficient Z gates for quantum computing, Phys. Rev. A **96**, 022330 (2017).
- [50] T. Adam *et al.* (OPERA Collaboration), Measurement of the neutrino velocity with the OPERA detector in the CNGS beam, J. High Energ. Phys. **2012**, 93 (2012).
- [51] European Organization For Nuclear Research and Open AIRE, Zenodo, CERN, 2021, <https://doi.org/10.5281/zenodo.13771265>
- [52] A. Ketterer, T. Wellens, Characterizing crosstalk of superconducting transmon processors, Phys. Rev. Applied **20**, 034065 (2023).
- [53] E. Weiss, M. Cech, S. Soltan, M. Koppenhöfer, Michael Krebsbach, Thomas Wellens, Daniel Braun, Pattern-based quantum functional testing, arXiv:2405.20828
- [54] R. Plaga, On a possibility to find experimental evidence for the many-worlds interpretation of quantum mechanics, Found. Phys. **27**, 559 (1997).
- [55] A. Bednorz, Objective realism and joint measurability in quantum many copies, Ann. Phys. **530**, 201800002 (2018).